Single cell immune profiling by mass cytometry of newly diagnosed chronic phase chronic myeloid leukemia treated with nilotinib

Stein-Erik Gullaksen,[1] Jørn Skavland,[1] Sonia Gavasso,[2,3] Vinko Tosevski,[4] Krzysztof Warzocha,[5] Claudia Dumrese,[6] Augustin Ferrant,[7] Tobias Gedde-Dahl,[8] Andrzej Hellmann,[9] Jeroen Janssen,[10] Boris Labar,[11] Alois Lang,[12] Waleed Majeed,[13] Georgi Mihaylov,[14] Jesper Stentoft,[15] Leif Stenke,[16] Josef Thaler,[17] Noortje Thielen,[10] Gregor Verhoef,[18] Jaroslava Voglova,[19] Gert Ossenkoppele,[10] Andreas Hochhaus,[20] Henrik Hjorth-Hansen,[21,22] Satu Mustjoki,[23,24] Sieghart Sopper,[25] Francis Giles,[26] Kimmo Porkka,[23] Dominik Wolf[25,27] and Bjørn Tore Gjertsen[1,28]

[1]Centre of Cancer Biomarkers CCBIO, Department of Clinical Science, Precision Oncology Research Group, University of Bergen, Norway; [2]Department of Clinical Medicine, University of Bergen, Norway; [3]Neuroimmunology Lab, Haukeland University Hospital, Bergen, Norway; [4]Mass Cytometry Facility, University of Zurich, Switzerland; [5]Department of Hematology, Institute of Hematology and Transfusion Medicine, Warsaw, Poland; [6]Flow Cytometry Facility, University of Zurich, Switzerland; [7]Hematology Department, Cliniques Universitaires St Luc, Brussels, Belgium; [8]Department of Medicine, Oslo University Hospital, Norway; [9]Department of Hematology, Medical University of Gdańsk, Poland; [10]Department of Hematology, VU University Medical Center, Amsterdam, the Netherlands; [11]Department of Hematology, University Hospital Center Rebro, Zagreb, Croatia; [12]Internal Medicine, Hospital Feldkirch, Austria; [13]Department of Hemato-Oncology, Stavanger University Hospital, Norway; [14]Clinic for Hematology, University Hospital Sofia, Bulgaria; [15]Hematology Unit, Aarhus University Hospital, Denmark; [16]Department of Medicine, Karolinska University Hospital, Stockholm, Sweden; [17]Department of Internal Medicine IV, Wels-Grieskirchen Hospital, Wels, Austria; [18]Department of Hematology, University Hospital Leuven, Belgium; [19]4th Department of Internal Medicine – Hematology, University Hospital Hradec Kralove, Czech Republic; [20]Department of Hematology and Medical Oncology, Universitätsklinikum Jena, Germany; [21]Department of Hematology, St Olavs Hospital, Trondheim, Norway; [22]IKM, NTNU, Trondheim, Norway; [23]Hematology Research Unit Helsinki, University of Helsinki and Helsinki University Hospital Comprehensive Cancer Center, Department of Hematology, Finland; [24]Department of Clinical Chemistry, University of Helsinki, Finland; [25]Department of Hematology and Oncology, Innsbruck Medical University and Tyrolean Cancer Research Institute, Innsbruck, Austria; [26]NMDTI, Robert H. Lurie Comprehensive Cancer Center of Northwestern University, Chicago, IL, USA; [27]Medical Clinic 3, Oncology, Hematology and Rheumatology, University Hospital Bonn (UKB), Germany and [28]Department of Internal Medicine, Haukeland University Hospital, Bergen, Norway

 doi:10.3324/haematol.2017.167080

Received: February 19, 2017.

Accepted: May 8, 2017.

Pre-published: May 18, 2017.

Correspondence: bjorn.gjertsen@med.uib.no

Supplementary Material

Single cell immune profiling by mass cytometry of newly diagnosed chronic phase chronic myeloid leukaemia treated with nilotinib

Table of contents: **Page**

Supplementary Material

1. Patient cohort, demographics and antibody panel

Longitudinally collected samples from a subset of patients enrolled in the Evaluating Nilotinib Efficacy and Safety as First-Line Treatment (ENEST1st)[1] (CAMN107EIC01) clinical trial were evaluated. An overview of patients analysed in the two datasets is shown in **Supplemental Table 1.**

Supplemental Table 1 – Overview of patients analysed by mass cytometry.

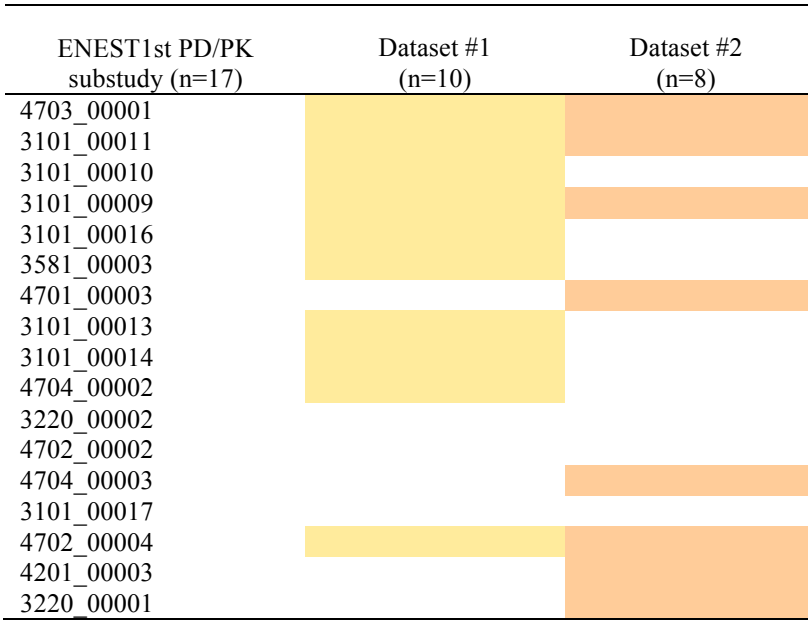

Supplemental Table 2 - Demographics and clinical data at diagnosis in ENEST1st PD/PK mass cytormetry substudy. Data for age, WBC, platelet counts, spleen size, Sokal and Euro scores are shown as medians with ranges in parenthesizes. Abbreviations: n, number; M, male; F, female; WBC, white blood cell counts.

	ENEST1st PD/PK substudy	Patient set #1	Patient set #2
n	17	10	8
Sex (M:F)	12:05	05:05	06:02
Age (years)	55 (34-68)	53 (34-68)	53.5 (40-59)
WBC (10^9/l)	81.43 (21.5-307)	98.15 (37.6-221)	72.62 (37.6-220)
Platelet count (10^9/l)	396 (98-1485)	491 (290-1485)	406 (144-822)
Spleen size (cm below costal margin)	0 (0-16)	3 (0-15)	2 (0-16)
Sokal score	0.83 (0.67-1.69)	1.11 (0.69-1.69)	0.76 (0.67-1.59)
Euro Score	912.4 (309.7-1774.9)	959.8 (309.7-1774.9)	919 (309.7-1773.4)

Supplementary Material

Supplemental table 3 – Final list of antibodies and reagents used for analysis of the second dataset.

#	Antibody	Clone	Mass Tag	Vendor
	Single Cell Metal Barcode			
1	MBC #1		102 Pd	Fluidigm
2	MBC #2		104 Pd	Fluidigm
3	MBC #3		105 Pd	Fluidigm
4	MBC #4		106 Pd	Fluidigm
5	MBC #5		108 Pd	Fluidigm
6	MBC #6		110 Pd	Fluidigm
	Cell surface markers			
7	CD45	Hi30	89 Y	Fluidigm
8	Caspase 3 (cleaved)	D3E9	142 Nd	Fluidigm
9	CD38	HIT2	144 Nd	Fluidigm
10	CD4	RPA-T4	145 Nd	Fluidigm
11	CD8	RPA-T8	146 Nd	Fluidigm
12	CD20	2H7	147 Sm	Fluidigm
13	CD16	3G8	148 Nd	Fluidigm
14	CD123	6H6	151 Eu	Fluidigm
15	CD66b	80H3	152 Sm	Fluidigm
16	CD56	B159	155 Gd	Fluidigm
17	CD11c	Bu15	159 Tb	Fluidigm
18	CD14	M5E2	160 Gd	Fluidigm
19	CD181	B-1	161 Dy	Santa Cruz
20	FoxP3	259D/C7	162 Dy	Fluidigm
21	CD193	5E8	163 Dy	Biolegend
22	CD34	581	166 Er	Fluidigm
23	CD182	E-2	168 Er	Santa Cruz
24	CD25	2A3	169 Tm	Fluidigm
25	CD3	UCHT1	170 Er	Fluidigm
26	HLA-DR	L243	174 Yb	Fluidigm
27	CXCR4	12G5	175 Lu	Fluidigm
28	CD11b	Mac-1	209 Bi	Fluidigm
Phospho-Specific Epitopes				
29	pBCR [Y177]	Polyclonal	141 Pr	Cell Signalling
30	pCRKL[Y207]	Polyclonal	143 Nd	Fluidigm
31	pSTAT5 [Y694]	47	150 Nd	Fluidigm
32	pSTAT1 [Y701]	58D6	153 Eu	Fluidigm
33	pAbl [Y245]	73E5	154 sm	Cell Signalling
34	pSTAT3 [Y705]	4/P-Stat3	158 Gd	Fluidigm
35	pCREB [S133]	87G3	165 Ho	Fluidigm
36	pERK 1/2 [T202/Y204]	D13.13.4E	171 Yb	Fluidigm
37	pS6 [S235/S236]	N7-548	172 Yb	Fluidigm
38	pS6 [S240/S244]	D68F8	176 Yb	Cell Signalling

2) Mass cytometry barcoding, staining and gating strategies.

A barcoding scheme was developed in-house for dataset #1 where each of the longitudinally collected patient, or healthy, peripheral blood (PB) samples was assigned, and stained with a single palladium isotope and subsequently pooled (**Supplemental Figure 1**). The PB samples from each patient collected before first dose of nilotinib, and after 3 hours, 7 days, and 28 days was stained with Pd 102, 104, 106 or 108, respectively.

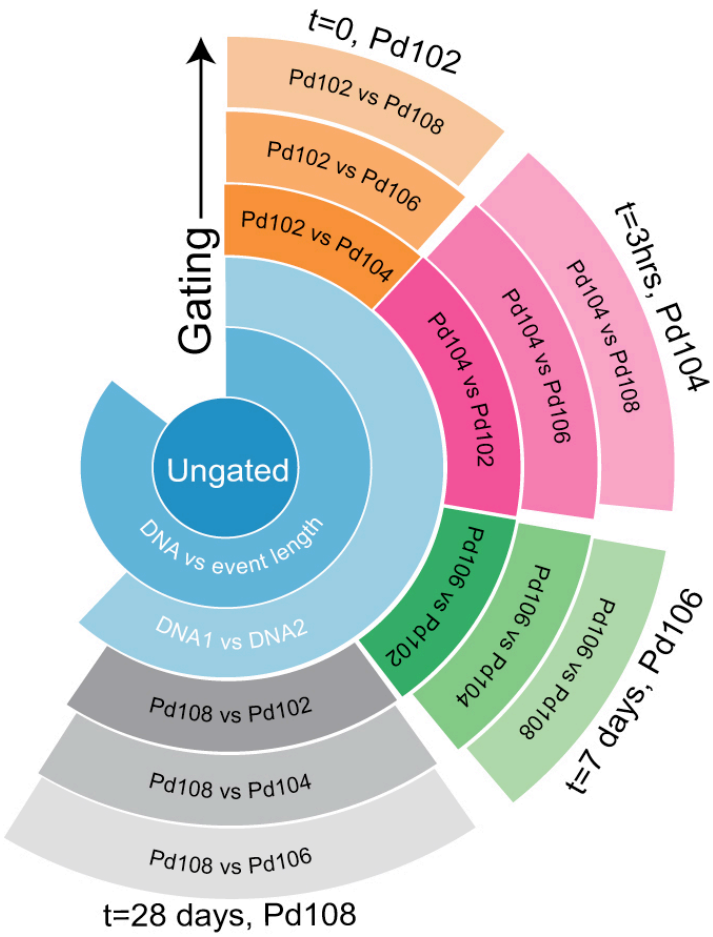

Supplemental Figure 1 - Gating each singularly palladium-stained sample (Pd102, Pd104, Pd106 or Pd108) against all other Pd isotopes allowed the deconvolution of the barcoded and pooled samples, and also further removal of cell doublets.

Supplementary Material

For dataset #2, a commercially available kit for barcoding was used (Fluidigm) according to manufacturers instructions[2]. Subsequently for both barcoding approaches, the pool of barcoded cells was stained with a panel of cell surface markers (30 minutes, RT), washed in Cell Staining Buffer (CSB, Fluidigm) and permeabilized with methanol (-20^{o}C). Further washing in CSB and staining with intracellular phospho-specific antibodies (30 minutes, RT) followed. Cells were then washed and re-suspended in Fix and Perm buffer (Fluidigm) with a 1:1250 dilution of iridium-intercalator (natural abundance iridium as pentamethylcyclopentadienyl-iridium (III)-dipyridophenazine, Fluidigm), for 1 hour at RT or over night at 4^{o}C. Immediately prior to data acquisition cells were washed once in CSB, twice in MaxPar water (Fluidigm), and re-suspended to a final concentration of approximately 5x10^{5} cells/mL in MaxPar water containing normalization beads (1:10 dilution, Fluidigm) and analysed on the mass cytometer (Fluidigm). Two sequential gating steps identified single cells. Firstly, all events were plotted on Ir191 *versus* event length. Then, further exclusion of cell doublets was achieved by stringent gating of cells plotted by the two Iridium isotopes against each other. De-barcoding the singularly palladium-stained samples, iteratively against all other palladium channels, identified the longitudinally collected patient samples, and further allowed doublet removal (**Supplemental Figure 1**). For samples barcoded with the commercially available barcoding kit (Fluidigm), the single cell debarcoder algorithm was used for sample deconvolution and further doublet removal (https://github.com/nolanlab/single-cell-debarcoder).

3. Antibody validation for dataset #1

We validated the specificity of the intracellular phospho-specific antibodies by exposing the CML blast phase cell line K562 *in vitro* to nilotinib (50 and 500 nM, 2 hours), interferon-α (HuINF-α-Le 2000 IU/mL, 15 min) or tert-butyl hydrogen peroxide (TBHP, 400 µM, 1 h). Nilotinib treated K562 cells were lysed and the pSTAT5 Y694, pCRKL Y207 and pBCR Y177 level measured by western blotting (**Supplemental Figure 2 – A**). In addition, the cells were stained with mass-tagged phospho-specific antibodies and changes in signal transduction were measured by mass cytometry and heat mapped as an arcsinh ratio of control and treated cells (**Supplemental Figure 2 – B**). To test both the surface and intracellular panels of antibodies on primary human material, newly aspirated healthy donor PB and BM were treated *in vitro* with 50 nM nilotinib for 3 hours. Cells were then preserved using an identical protocol used for sample collection within the ENEST1st study[1]. To reduce the sample-to-sample variation and antibody consumption, all samples were barcoded and pooled before antibody staining (in-house barcoding approach). After acquisition of data, doublet removal and barcode deconvolution, the cellular subsets were identified by manual annotation of the SPADE algorithm[3] generated tree structures of clustered high dimensional data. As depicted in **Supplemental Figure 2 - C and D**, SPADE generated tree structures allowing the identification of specific cellular subsets in both PB and BM samples. Both healthy PB and BM samples were treated *in vitro* with nilotinib (50 nM, 3 hours), and the heat maps in **Supplemental Figure 2 - C and D** shows induced changes in signal transduction. Only modest alterations in phosphorylation levels were measured. However, we identified a down-regulation of several epitopes in the healthy control PB sample, including pAbl Y245, pCrKL Y207 and pSTAT5 Y694 in several populations (i.e. activated T cells, CD8 T cells, neutrophils and basophils).

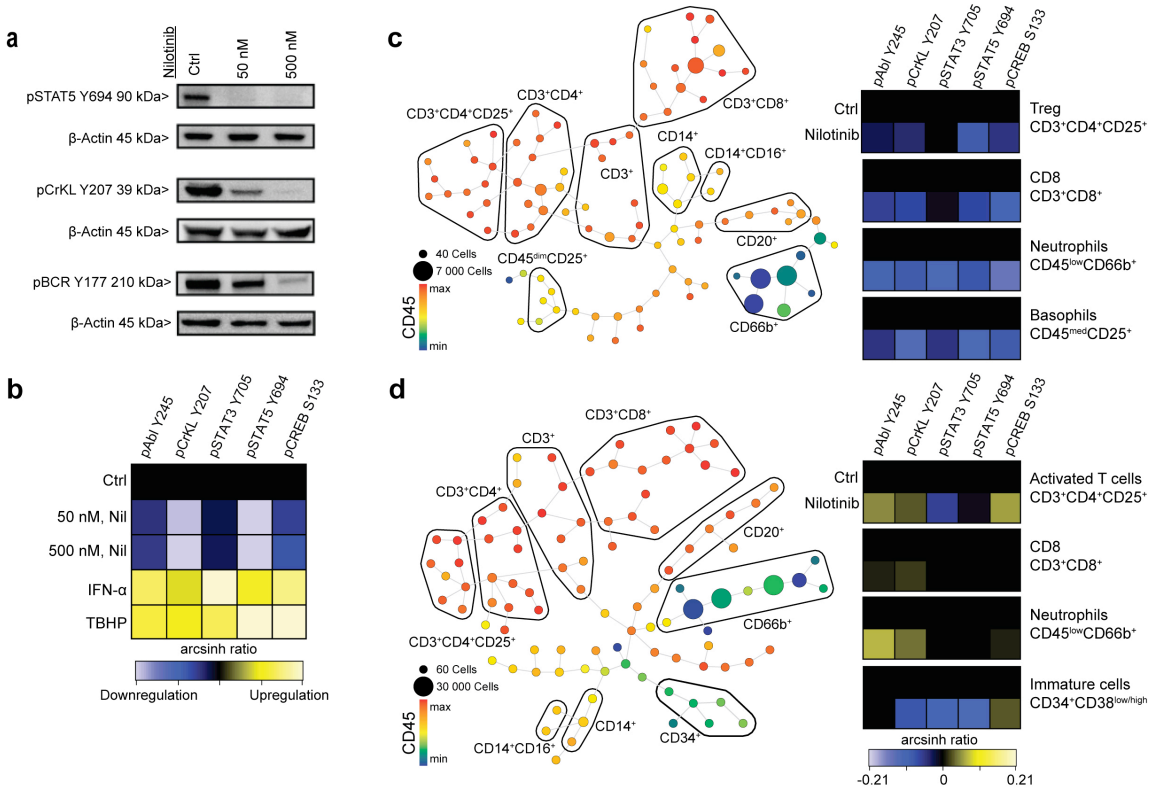

Supplemental Figure 2 - Validation of mass cytometry assay in healthy peripheral blood, bone marrow and in a CML cell line. K562 cells were treated *in vitro* with nilotinib (**Nil**, 50 and 500 nM, 2h), interferon-α (**IFN-α**, 2000 IU/mL, 15 min) and tert-butyl hydrogen peroxide (**TBHP**, 400 µM, 1 h). **a)** Nilotinib treated K562 cells were lysed and pSTAT5 Y694, pCrKL Y207 and pBCR Y177 level was measured by the Western Blotting technique. **b)** Treated K562 samples were stained with mass-tagged phospho-specific antibodies and changes in signal transduction were measured by mass cytometry and heat mapped as an arcsinh ratio of control and treated cells**.** Healthy donor peripheral blood (**c**) and bone marrow (**d**) from a single donor was collected and immediately treated *in vitro* with 50 nM nilotinib for 3 hours. In **c)** and **d)**, the SPADE algorithm[3] was used to cluster cells. The size of each node corresponds to the number of cells clustered, and the expression of CD45 is color-coded from minimum (blue) to maximum (red). Intracellular signalling data was exported for each subpopulation and heat mapped as an arcsinh ratio of treated cells compared to control cells.

The functionality of the panel was also validated by analysing PB leukocytes from 4 healthy donors and a complete set of longitudinal PB samples from two patients (patients # 4810-00004 and 4810-00005, at diagnosis, and after 3 hours, 7 days and 28 days of therapy) enrolled in the ENEST1st study[1]. Single cell data from the four healthy PB

samples, and the two longitudinal sets of patient samples were each pooled and analysed using the SPADE algorithm[3] (**Supplemental Figure 3**). The manually annotated SPADE trees populated with the samples collected from CML patients identified 9 cellular subsets; neutrophils ($CD66b^{+}CD45^{dim}$), monocytes ($CD14^{+}$), B Cells ($CD20^{+}$), Cytotoxic T cells ($CD3^{+}CD8^{+}$), T Helper cells ($CD3^{+}CD4^{+}$), double negative T cells ($CD3^{+}CD8^{-}CD4^{-}$), activated T cells ($CD3^{+}CD4^{+}CD25^{+}$), hematopoietic progenitor cells ($CD34^{+}CD38^{Low/high}$) and finally a highly defined branch of CD25 positive cells. Although CD25 is not a canonical marker for basophils, the expression of CD25, together with a CD45 expression slightly lower than lymphocytes, was used to delineate the basophil cell population[4]. The relative frequencies of different cell populations, at before start of treatment and after 28 days of treatment, was averaged for the two patients and compared to the average of the four healthy donors (**Supplemental Figure 3 - B**). We observed a relative expansion of the lymphocyte compartment after 28 days of treatment, illustrating normalization of PB during TKI therapy. This was also consistent for the myeloid cell populations, as mirrored by a clear compression of immature $CD34^{+}$ cells and $CD25^{+}$ basophils. Phospho-specific signalling measured in longitudinal patient samples were plotted in heat maps as arcsinh ratios relative to the averaged profile of the four healthy samples (**Supplemental Figure 3 - C**). We observed a clearly different state of signalling between the cellular subsets of the healthy donor averages and the two sets of longitudinal patient samples. In the two T cell populations and the basophils, an increased level of phosphorylation of pAbl Y245 and pCRKL Y207 was seen. Of note, the phosphorylation level of pSTAT3 Y694 in the neutrophil compartment was attenuated, which recovered to normal after 28 days of TKI therapy.

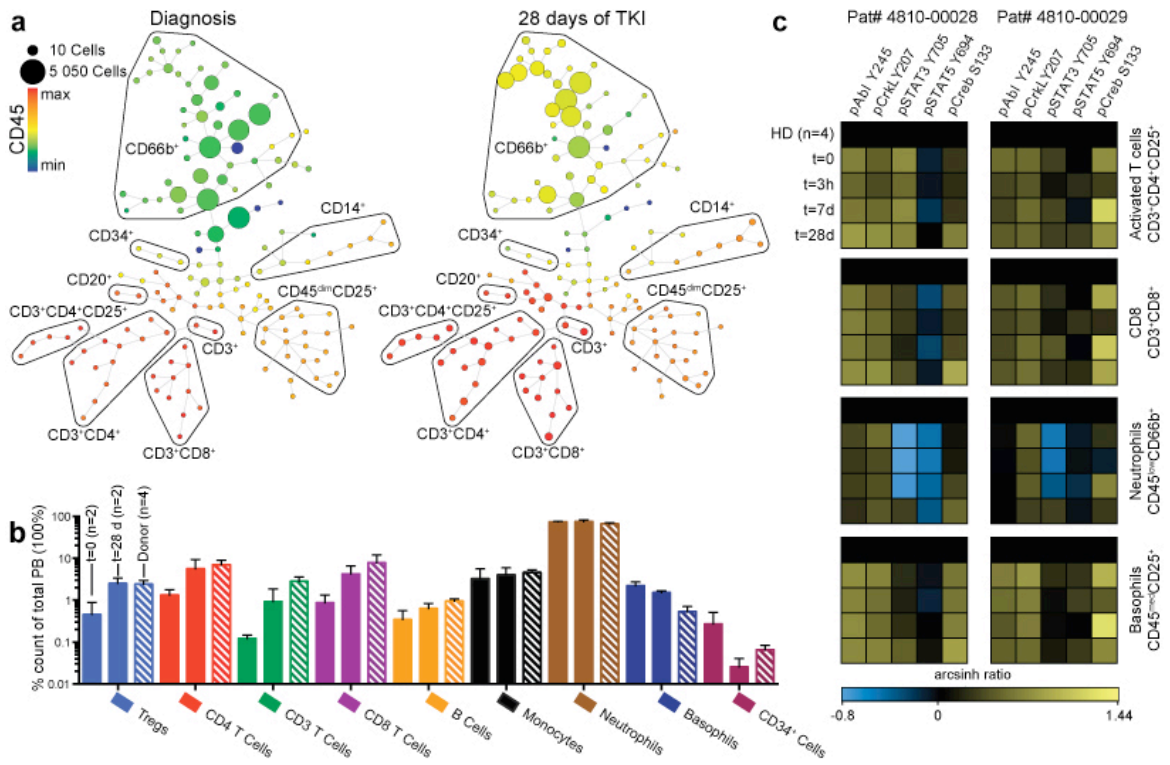

Supplemental Figure 3 – Longitudinal samples from chronic phase CML patients treated with nilotinib analysed by mass cytometry. PB from four healthy donors and the longitudinal samples from two patients (# 4810-0004 and 4810-005) collected before (t=0), and after 3 hours (t=3h), 7 days (t=7d) and 28 days (t=28d) of treatment, enrolled in ENEST1st study was investigated. **a**) The longitudinal samples from each patient, and healthy donors, were each pooled and clustered using the SPADE algorithm[3]. The figure shows the manually annotated SPADE tree of pat# 4810-0004 populated with the sample collected at diagnosis and after 28 days of therapy. The size of each node represents the number of cells clustered and the expression of CD45 is color-coded. **b**) For the different hematopoietic lineages, the averaged relative frequency of cells calculated from patient samples (solid bars, n=2) collected before and after 28 days are plotted and compared to the average frequencies of healthy donors (hatched bars, n=4, the error bars show SEM). There was no node readily identifiable as a $CD34^+$ population in the PB samples from the four healthy donors. By expert manual gating, the mean percentage of $CD34^+$ cells was found to be 0.0652 % (range: 0.0441-0.0863%), which is within the normal range. **c**) To evaluate differences at diagnosis, and subsequent changes in signal transduction as a function of therapy, the 75^{th} percentile intensity of signalling substrates of the time resolved patient samples was heat mapped relative to the average of healthy donors (n=4), using an arcsinh ratio.

4. Extended antibody validations for dataset #2

4.1 Additional cell surface markers

To further increase the immunophenotyping resolution of the myeloid lineage, the antibody panel was extended with a selection of carefully chosen cell surface markers. This panel was then used to investigate the diagnostic PB samples collected from three ENEST1st trial[1] patients (4303-00003, 3101-00011 and 3581_00002) and a single healthy donor PB sample. We performed a data-driven analysis of the generated high dimensional data using the PhenoGraph algorithm[5]. The PhenoGraph algorithm clustered each sample into an average of 27.5 cellular subsets (termed centroids, ranging from 24 to 33, 110 in total) based on the expression of 18 cell surface markers. To identify and compare similar cellular subsets between samples, we performed a meta-cluster analysis across the pooled centroids from all four samples. The algorithm returned 17 meta-clusters (MCs), where each meta-cluster contained centroids (cells) from any number of samples. In **Supplemental Figure 4**, the heat map shows the normalized expression profile of all 18 cell surface markers across all the identified 17 MCs. Of the 17 MCs identified, 13 MCs contained cells from the healthy donor sample (MC: 1-7, 9 and 11-15), indicating that MC-8, -10, -16 and -17 represent a disease specific phenotype (see bar chart, **Supplemental Figure 4**). These putative CML specific MCs are all $CD66b^{+}CD45^{low}$ cells, with varying expression levels of CD16 and CD10. Additionally, MC-13 is almost exclusively made up of patient cells at diagnosis, indicating a measured expansion of this cellular subset in the diagnostic samples. The clustered cells in MC-13 are $CD45^{med}HLA\text{-}DR^{-}CD25^{+}CD123^{+}$ a phenotype consistent with basophils.

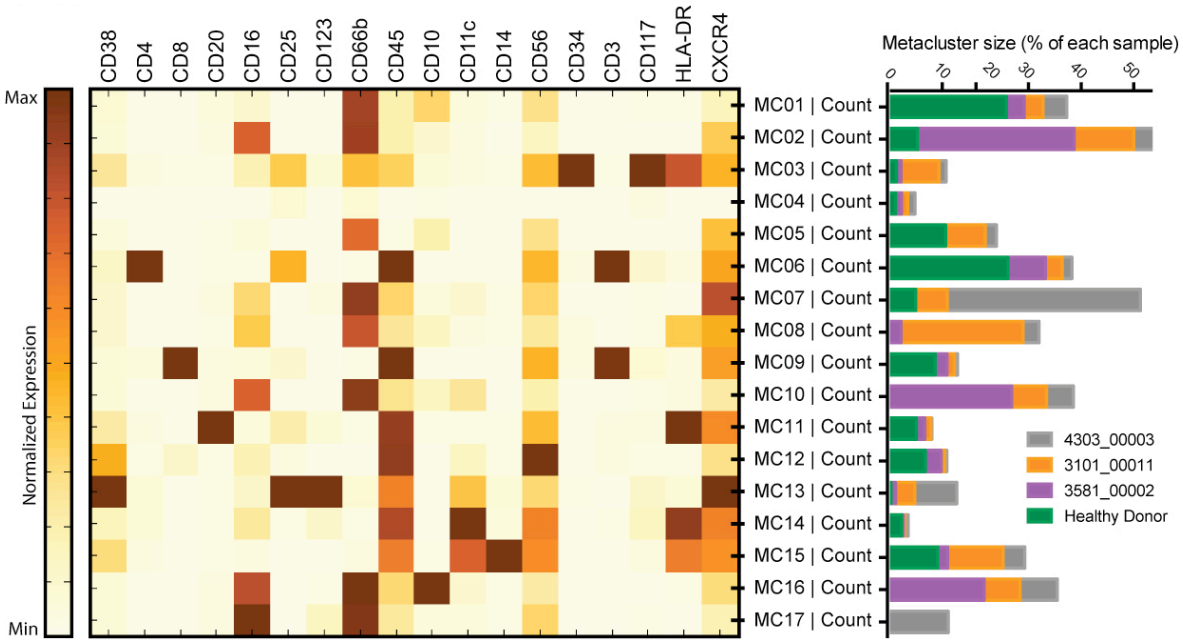

Supplemental Figure 4 - Data-driven discovery of cellular subsets in CML and healthy peripheral blood. Three collected before treatment initiation (4303-00003, 3101-00011 and 3581-00002) and one healthy donor sample were analysed using the PhenoGraph algorithm[5]. The algorithm creates several clusters of phenotypically similar cells in each of the four samples. Then, by performing a meta-cluster analysis, similar clusters across samples are clustered together, into meta-clusters (**MCs**). Here, the meta-cluster analysis produced 17 MCs, where each MC is comprised of similar clusters that may be from any number of samples. The phenotype of the 17 MCs is shown in the heat map, where the expression of cell surface markers are normalized and color-coded. This heat map creates an overview of the distinct immunophenotypes identified by the algorithm. The relative abundances of the different samples within each MC are plotted in the horizontal bar chart.

4.2 Additional intracellular phospho-specific antibodies to expand the single cell profile resolution

To add more dimensions in the mass cytometric analysis, we included antibodies against key signal transduction substrates known to be involved in the Bcr-Abl1 signalling[6,7]. To ensure the specificity of our panel of antibodies targeting intracellular signal transduction, we developed a repository of cell lines treated with agents activating or inhibiting key intracellular signal transduction pathways. The CML cell line K562 cells were treated with dasatinib (1 μM, 2h) and nilotinib (500 nM, 2h); Jurkat cells were treated with PMA (1μM, 15 min), U0126+PMA (10 μM, 30 min, then PMA as above), FBS (10 %, 15 min), BEZ235 + FBS (200 nM, 30 min, then FBS as above); and U937 cells treated with GM-CSF (20 ng/mL, 15 min), IL-4 (20ng/mL, 15 min), IFN-α (10 ng/mL, 15 min), TNF-α (20 ng/mL, 15 min) and finally FBS (10 %, 15 min). The induction of signal transduction was verified using conventional flow cytometry (**Supplemental Figure 5 - A**). Treated cells, and untreated control cells, were barcoded, pooled and the changes in intracellular signal transduction were measured on the mass cytometer (**Supplemental Figure 5 - B**).

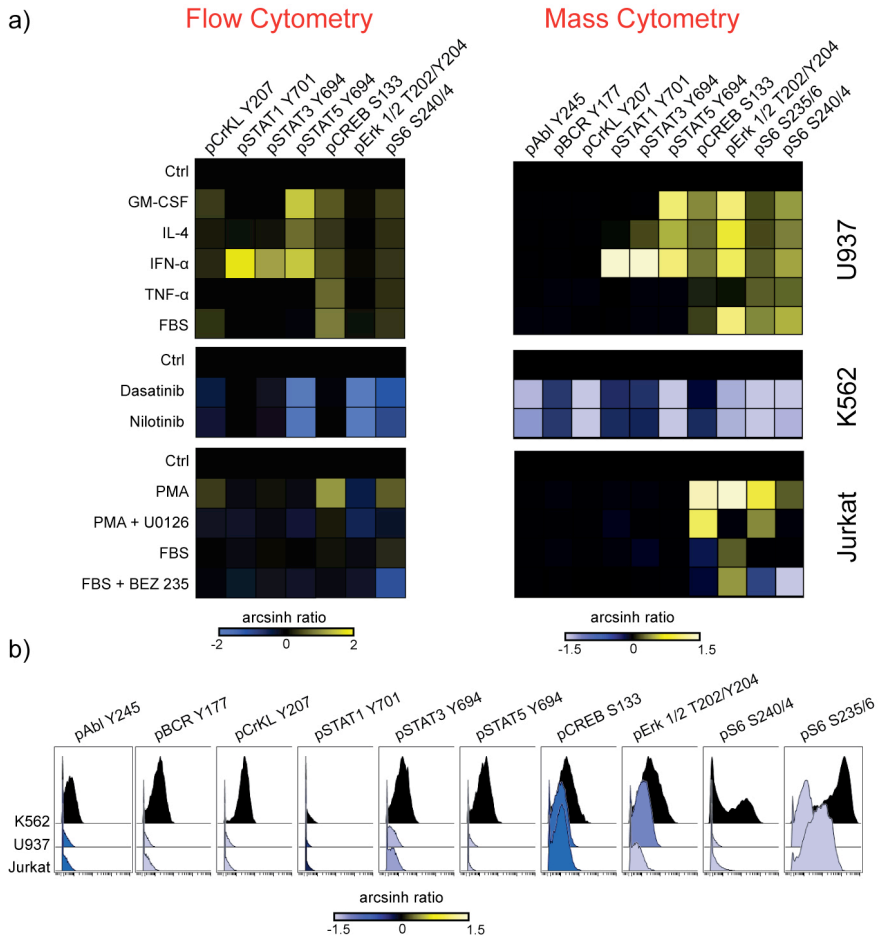

Supplemental Figure 5 – Verification of phospho-specific antibodies. a) The induction of changes in signal transduction in stimulated cell lines was verified using conventional Flow Cytometry. **b**) This material was then used to validate the intracellular phospho-specific antibodies for mass cytometry. Arcsinh ratio was calculated to compute changes in signal transduction, and the scale was adjusted to ±1.5 to improve resolution. **C**) Histograms show the baseline variation between the cell lines, relative to K562.

In the CML blast phase cell line K562, both dasatinib and nilotinib down-regulated the phosphorylation of pBCR Y177 and pAbl Y245, but also the signalling substrates of Bcr-Abl1; pCRKL Y207 and pSTAT5 Y694. Furthermore indicating antibody specificity, the basal phosphorylation level (in untreated cells) of pBCR Y177, pAbl Y245, pCRKL Y207 and pSTAT5 Y694, interestingly pCREB S133, was clearly elevated in K562 cell line compared to the two other non-CML cell lines (**Supplemental Figure 5 - B**).

5. Supporting data for dataset #2

A second cohort of patients (n=8) from the ENEST1st study was analysed to evaluate the robustness of the assay and to examine nilotinib-induced changes in intracellular signal transduction of possible prognostic value. Single cell clustering by SPADE analysis (**Figure 2**) the longitudinally collected patient PB samples and healthy donor PB identified several cellular subsets, including T helper cells ($CD3^+CD4^+$), activated T cells ($CD3^+CD4^+CD25^+$), T regulatory cells ($CD3^+CD4^+CD25^+PoxP3^+$), cytotoxic T cells ($CD3^+CD8^+$), double negative T cells ($CD3^+CD8^-CD4^-$), monocytes ($CD14^+$), B cells (HLA-DR^+CD20^+), basophils ($CD45^{med}$HLA-$DR^-CD123^+CD25^+$), DC cells (HLA-DR^+CD11c^+), pDC cells (HLA-DR^+CD123^+), NK cells (HLA-DR^-CD56^+), hematopoietic stem and progenitor cells ($CD34^+CD38^{Low/high}$), neutrophils ($CD45^{dim}CD66b^+$ $CD16^+$) and finally myelocytes ($CD45^{dim}CD66b^+$ $CD16^-$).

Some cellular subsets were identifiable only in some of patients.

We measured the 75th percentile of each intracellular phosphor-specific target (pBcr Y177, pAbl Y245, pCrKL Y207, pSTAT1 Y701, pSTAT3 Y705, pSTAT5 Y694, pCREB S133, pErk ½ T202/Y204, pS6 S235/36 and pS6 S240/44) in the subsets (**Figure 3**). The arcsinh ratio between before treatment initiation and both after 3 hours and 7 days in each population was calculated. The patient cohort (n=8) was divided into two groups based on the BCR-ABL1^{IS} at 3 and 6 months (best and worst initial responders to nilotinib). The arcsinh ratio between before treatment initiation and both after 3 hours and 7 days is shown for these two groups in **Supplemental Figure 6**. This arcsinh ratio data was used to perform the PCA analysis in **Figure 3**.

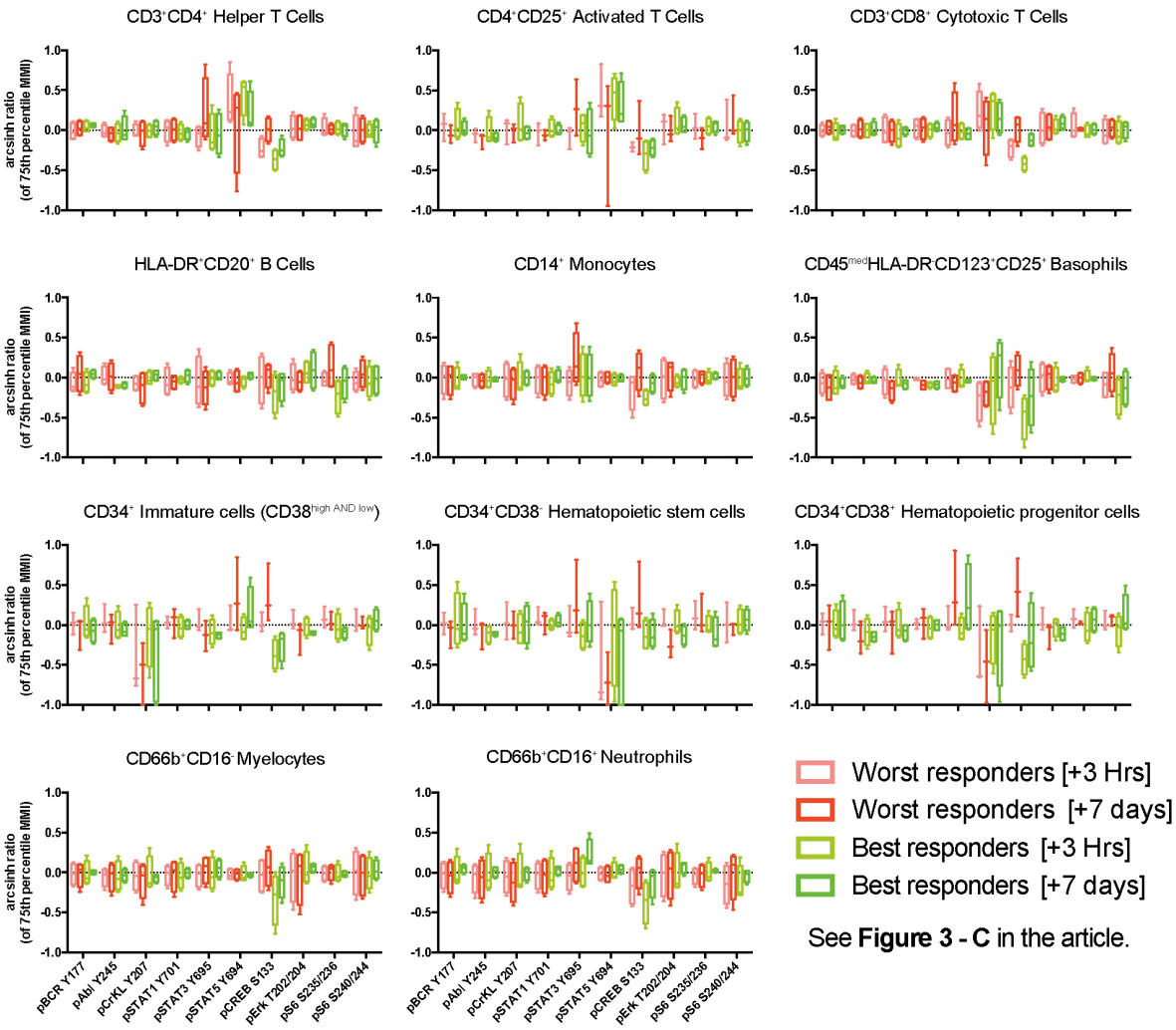

Supplemental material figure 6 – Modulation of intracellular phospho-proteins as a function of nilotinib therapy. The cohort of 8 patients were split into two groups based BCR-ABL1^{IS} at 3 and 6 months (low in green and high in red). The arcsinh ratio was calculated in the longitudinal samples collected before treatment initiation and both after 3 hours and 7 days of nilotinib therapy.

Supplementary Material

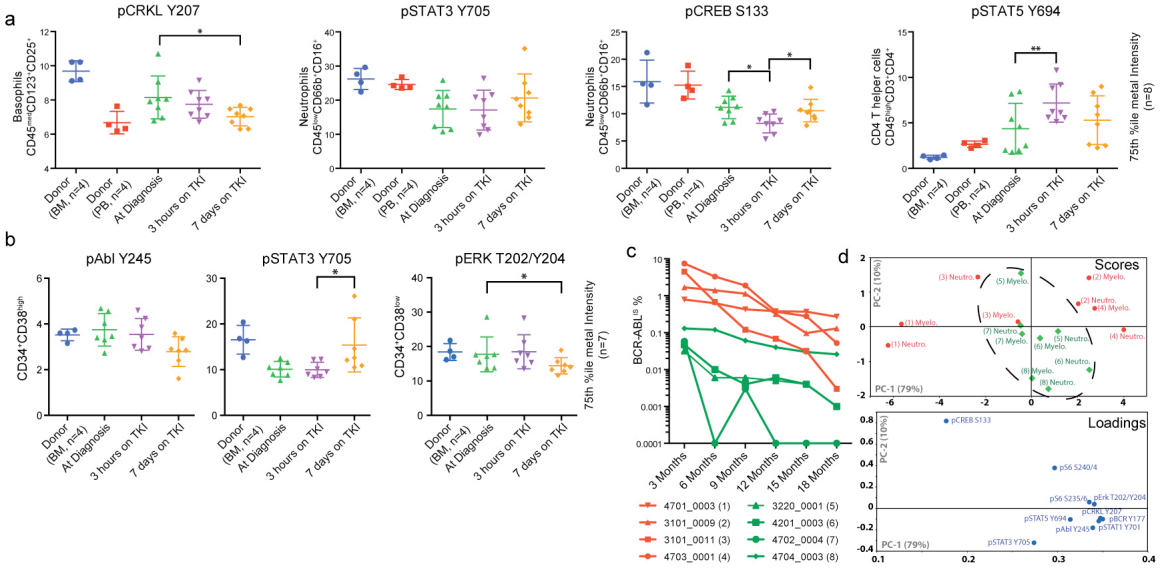

Supplemental material figure 7 – Single cell signal transduction in nilotinib-treated CML patient cellular subsets correlate to BCR-ABL1 molecular response. The figure presents the same data as **Figure 3** in the manuscript. But the data in in panels **a)** and **b)** is visualized as scatter dot plots with mean and SD.

6. References

1. Hochhaus A, Rosti G, Cross NC, Steegmann JL, le Coutre P, Ossenkoppele G *et al.* Frontline nilotinib in patients with chronic myeloid leukemia in chronic phase: results from the European ENEST1st study. *Leukemia* 2015 2016;**30**:57-64.

2. Zunder ER, Finck R, Behbehani GK, Amir el-AD, Krishnaswamy S, Gonzalez VD *et al.* Palladium-based mass tag cell barcoding with a doublet-filtering scheme and single-cell deconvolution algorithm. *Nat Protoc* 2015;**10**:316-333.

3. Qiu P, Simonds EF, Bendall SC, Gibbs KD Jr, Bruggner RV, Linderman MD *et al.* Extracting a cellular hierarchy from high-dimensional cytometry data with SPADE. *Nat Biotechnol* 2011;**29**:886-891.

4. Han X, Jorgensen JL, Brahmandam A, Schlette E, Huh YO, Shi Y *et al.* Immunophenotypic study of basophils by multiparameter flow cytometry. *Arch Pathol Lab Med* 2008;**132**:813-819.

5. Levine JH, Simonds EF, Bendall SC, Davis KL, Amir el-AD, Tadmor MD *et al.* Data-Driven Phenotypic Dissection of AML Reveals Progenitor-like Cells that Correlate with Prognosis. *Cell* 2015;**162**:184-197.

6. Deininger MW, Goldman JM, Melo JV. The molecular biology of chronic myeloid leukemia. *Blood*. 2000;**96**:3343-56.

7. Cilloni D, Saglio G. Molecular pathways: BCR-ABL. *Clin Cancer Res*. 2012;**18**:930-7.